# Preparation and Structure Analysis of Co−Mo Binary Sulfide Clusters Encapsulated in an NaY Zeolite

**Yasuaki Okamoto,*,† Hidenori Okamoto,† Takeshi Kubota,† Hisayoshi Kobayashi,‡ and Osamu Terasaki§**

*Department of Material Science, Shimane University, Matsue 690-8504, Japan, Department of Chemical Technology, Kurashiki University of Science and the Art, Kurashiki 712-8505, Japan, and CREST, Department of Physics, Tohoku University, Sendai 980-8578, Japan*

*Received: March 24, 1999; In Final Form: June 4, 1999*

In our previous study, it was proposed that thermally stable intrazeolite Co−Mo binary sulfide clusters were synthesized using as precursors $Mo(CO)_6$ and $Co(CO)_3NO$ adsorbed in the pores of an NaY zeolite. In the present study, the formation of Co−Mo binary sulfide clusters is shown by Co 2p X-ray photoelectron spectroscopy (XPS) and Mo and Co K-edge extended X-ray absorption fine structure (EXAFS) techniques. It is concluded on the basis of XPS and X-ray fluorescence (XRF) analyses that the composition of the clusters is $Co_2Mo_2S_6$. It is strongly suggested by Mo and Co K-edge EXAFS analysis that the structure of $Co_2Mo_2S_6$ clusters is of thiocubane type. The thiocubane structure is rationalized by theoretical calculations using a density functional method. It is concluded that the intrazeolite Co−Mo binary sulfide clusters $Co_2Mo_2S_6$, possessing a thiocubane structure thermally stabilized by interactions with the framework of the host zeolite, are synthesized by using $Mo(CO)_6$ and $Co(CO)_3NO$. Analogies in the synthesis reactions of Co−Mo thiocubane clusters are suggested between homogeneous reaction systems and the present zeolite pore system.

## Introduction

Alumina-supported Co(Ni)−Mo sulfide catalysts have been industrially employed for hydrodesulfurization (HDS) reactions of organic sulfur compounds in petroleum feedstocks.[1,2] Numerous studies[2−8] were conducted to understand the structure of catalytically active phases, the reaction mechanism of HDS, and the origin of catalytic synergy between Co(Ni) and Mo sulfides. A so-called "Co−Mo−S model", where Co decorates the edges of $MoS_2$ crystallites, proposed by Topsøe et al.[2,3,9] for catalytically active phases attracts increasing attention to explain many aspects of catalytic and spectroscopic properties. However, because of heterogeneity inherent to practical Co(Ni)−Mo sulfides supported on $Al_2O_3$ or activated carbon, precise structures of the active sites and, in particular, HDS reaction mechanisms are still ambiguous.[2−8] Better understanding of the nature of Co(Ni)−Mo sulfide catalyst systems is of great importance for a rational design of highly active HDS catalysts.

One of the promising approaches for these purposes is to utilize homogeneous molecular clusters as model catalysts in homogeneous or heterogeneous reaction systems. In both reaction systems, several attempts were reported for Co−Mo binary sulfide clusters and related catalyst systems.[5,10−19] Curtis et al.[13] showed with a homogeneous reaction system that a Co−Mo binary sulfide cluster **1**, $Cp'_2Mo_2Co_2S_3(CO)_4$ ($Cp' = \eta^5$-$C_5H_4Me$), desulfurizes at 387−423 K organic sulfur compounds, such as *t*-BuSH, $Me_2CHCH_2CH_2SH$, PhSH, and thiophene, to form organic moieties and a cubane cluster **2**, $Cp'_2Mo_2Co_2S_4(CO)_2$, in high yield. However, it was unsuccessful to construct a catalytic cycle using cluster **1**, since cluster **2** did not react with a mixture of $H_2$ (8 atm) and CO (32 atm) at 423 K. Increasing the CO pressure to 69 atm gave a 20% conversion of **2** to the original cluster **1** and COS. A combination of the desulfurization of thiophene and conversion of **2** to cluster **1** was unsuccessful even in the presence of 69 atm of CO and 15 atm of $H_2$, and the starting materials were recovered at 423 K. However, it was shown[15] that the HDS of cyclopropylmethanethiol using cluster **1** gives products identical with those over a sulfided $Co-Mo/Al_2O_3$ conventional HDS catalyst. This demonstrates that cluster **1** can be a model cluster of the practical catalysts. Despite stoichiometric reactions, the desulfurization using cluster **1** provides important information relevant to the reaction mechanism of HDS: a nucleophilic attack of a sulfur compound on the Co sites of cluster **1** followed by Co−S−Mo bond formation and desulfurization.[13−15]

Co−Mo binary sulfide clusters were employed as precursors for the preparation of supported Co−Mo sulfide catalysts.[17−19] However, molecular structures of the supported Co−Mo and Fe−Mo binary sulfide clusters were significantly modified by interactions with the supports and during HDS reaction at an elevated temperature and, accordingly, was not defined well as the model catalysts.[18] Synthesis of uniform Co−Mo binary sulfide clusters thermally stabilized on the support is desirable for these purposes.

In a previous study,[20] we proposed the formation of Co−Mo binary sulfide clusters thermally stabilized in NaY zeolite cages mainly on the basis of the catalytic properties. The intrazeolite clusters showed a high thiophene HDS activity at 623 K even at a low $H_2$ pressure. In the present study, the formation and structure of a novel type of intrazeolite Co−Mo binary sulfide clusters are investigated using extended X-ray absorption fine structure (EXAFS) and X-ray photoelectron spectroscopy (XPS). Theoretical calculations based on a density functional (DF)

* To whom correspondence should be addressed. Fax: +81-852-32-6429. E-mail: yokamoto@riko.shimane-u.ac.jp.
† Shimane University.
‡ Kurashiki University of Science and the Art.
§ Tohoku University.

10.1021/jp990999g CCC: $18.00 
Published on Web 08/06/1999

method are also carried out to examine the structure experimentally derived from EXAFS analyses.

## Experimental Section

**Preparation Methods of Intrazeolite Metal Sulfide Clusters**. After evacuation at 673 K for 1 h (ca. $1 \times 10^{-3}$ Pa), an NaY zeolite (Si/Al = 2.5, Catalyst and Chemicals Ind., Japan) was exposed to a vapor of $Mo(CO)_6$ for 16 h at room temperature (RT) followed by evacuation for 10 min at RT to remove physisorbed $Mo(CO)_6$ on the external surface of the zeolite. The amount of immobilized $Mo(CO)_6$ was two molecules per supercage (SC) of the zeolite according to chemical analysis. $Mo(CO)_6$/NaY was sulfided in a stream of 10% $H_2S/H_2$ (200 $cm^3$ $min^{-1}$, atmospheric pressure). The sulfidation temperature was increased from RT to 373 K at a rate of 2 K $min^{-1}$ and kept isothermal at 373 K for 1 h. Subsequently, the temperature was ramped to 673 K at a rate of 5 K $min^{-1}$ and kept at 673 K for 1.5 h. After the sulfidation, the sample was cooled in the $H_2S/H_2$ stream to RT and then evacuated at 673 K for 1 h. The Mo sulfide catalyst thus prepared is denoted MoSx/NaY. MoSx/NaY was exposed to a vapor of $Co(CO)_3NO$ for 15 min at RT. Saturation (two molecules of $Co(CO)_3NO$ per SC) was attained within a few minutes. After evacuation at RT for 10 min, $Co(CO)_3NO$/MoSx/NaY was sulfided at 673 K for 1.5 h in a 10% $H_2S/H_2$ stream in a manner identical with that for $Mo(CO)_6$/NaY. The sample was denoted CoSx−MoSx/NaY. CoSx−MoSx/NaY sulfided for 20 h in the stream of $H_2S/H_2$ at 673 K was also prepared. CoSx/NaY was prepared by sulfiding $Co(CO)_3NO$/NaY at 673 K for 1.5 h.

As a precursor of Co sulfide, $Co_2(CO)_8$ was used in the preparation of a Co−Mo sulfide catalyst instead of $Co(CO)_3NO$. $Co_2(CO)_8$ dispersed in degassed *n*-heptane was admitted to MoSx/NaY in a vacuum through a breakable joint while shaking well. The amount of $Co_2(CO)_8$ added was equivalent to 2.0 Co/SC. After removal of the solvent by evacuation at RT, $Co_2(CO)_8$/MoSx/NaY was sulfided at 673 K for 1.5 h in the same fashion as CoSx−MoSx/NaY. The catalyst sample prepared using $Co_2(CO)_8$ is denoted CoSx/MoSx/NaY. The Co and Mo content of the sulfided catalysts was determined by chemical analysis (atomic absorption spectroscopy (AAS) and inductively coupled plasma (ICP) spectroscopy) with an accuracy of ±0.1 atom/SC.

For the sake of the elemental analysis of the sulfide samples, X-ray fluorescence (XRF; Rigaku Industrial Corp., RIX3001) measurements were conducted under a He stream to minimize degradation of the sulfide sample during the XRF analysis. Polycrystalline $Co_9S_8$ and $MoS_2$ were used as reference compounds.

**Physicochemical Characterizations**. The Mo and Co K-edge EXAFS spectra of the sulfide samples and reference compounds were measured on the BL-10B (Si(311) double-crystal monochromator) and 12C (Si(111) double-crystal monochromator) stations, respectively, at the Photon Factory of the National Laboratory for High Energy Physics by means of synchrotron radiation. The EXAFS spectra were obtained at RT in transmission mode (Mo and Co K-edges) or fluorescence mode (Co K-edge) using an in situ cell with Kapton windows. The experimental EXAFS spectra were analyzed using a computer program supplied by Technos Co. Ltd. (Japan). Background below the edge jump was subtracted by using a Victreen polynomial with an added constant through the preedge region. Background above the EXAFS region was determined by fitting a cubic spline through three data segments. The EXAFS data were analyzed using the FEFF codes (version 6.0) developed by Rehr et al.[21] The theoretical phase shifts and backscattering amplitudes were calculated for single scattering absorber (Mo, Co)−backscatterer (S, Mo, Co) pairs. A spherical wave approximation was used in the calculations of the structural parameters using the theoretical EXAFS parameters thus obtained. The accuracy of the bond distances was ±0.002 nm. The coordination numbers were determined to within about 20%.

X-ray photoelectron spectra (XPS) of sulfided catalysts were measured on a ESCALAB 220i (VG) photoelectron spectrometer using Al $K\alpha_{1,2}$ radiation (1486.6 eV, 600 W). The catalyst samples were mounted on double-sided adhesive tape in a glovebox filled with Ar of high purity (6 N) followed by evacuation at RT in a pretreatment chamber ($1 \times 10^{-7}$ Pa) prior to the XPS measurements. The binding energies were referenced to the Si 2p level at 103.1 eV for the NaY zeolite as an internal standard, whose value was separately determined by using the C 1s level at 285.0 eV due to adventitious carbon. The accuracy of the binding energies was ±0.2 eV.

**Theoretical Calculation Method and Models**. The linear combination of Gaussian type orbital (LCGTO) DF program deMon was used throughout the calculations.[22] The orbital basis sets used in the calculations are described as [633321/53211/531], [63321/531/41], and [311/211/1] for Mo, Co, and S atoms, respectively, as summarized in Table 1S in Supporting Information. The all-electron bases were used for Mo and Co atoms, but the model core potential basis was used for S atoms. The Coulomb potential and exchange−correlation potentials were fitted by the auxiliary Gaussian functions. All the calculations were carried out using the gradient-corrected functionals of Becke's exchange[23] and Perdew's correlation.[24] The structure of $Co_2Mo_2S_6$ thiocubane clusters shown below was optimized under the symmetry constraint of $C_{2v}$.

## Results and Discussion

The location and dispersion of Mo sulfide species in MoSx/NaY (2 Mo/SC) were studied in our previous work[25] by EXAFS, XPS, X-ray diffraction (XRD), and high-resolution transmission electron microscopy (TEM) techniques and pore volume measurements. It was revealed that the zeolite framework is not destroyed at all by the incorporation of $Mo(CO)_6$ and subsequent sulfidation and that Mo sulfide clusters are located inside the supercage of the zeolite.

Shown in Figure 1 are the $k^3$-weighted Mo K-edge EXAFS oscillation and Fourier transform for MoSx/NaY (2 Mo/SC). The best fit of Fourier filtered EXAFS function is also presented in Figure 1. The structural parameters of MoSx/NaY as derived from the EXAFS analyses by using empirical[22] and theoretical EXAFS parameters are compared in Table 1. Both structural parameters are in fairly good agreement with each other. On the basis of the Mo−Mo coordination number (ca. 1), it is concluded that Mo sulfide clusters are highly dispersed, possibly forming Mo dimer species. Figure 2 shows the $k^3$-weighted Co K-edge EXAFS oscillation and Fourier transform for CoSx/NaY (2 Co/SC). The results of curve-fitting of Fourier filtered EXAFS oscillation are also presented in Figure 2. The EXAFS results in Table 1 for CoSx/NaY show that the coordination number of Co−Co bondings is about unity, suggesting an extremely high dispersion of Co sulfide species, possibly Co sulfide dimer species. Contributions of Mo−O or Co−O bondings could not be explicitly confirmed by the present EXAFS analysis of MoSx/NaY and CoSx/NaY. The formation of Mo and Co sulfide dimer species may be rationalized by the fact that two $Mo(CO)_6$ or $Co(CO)_3NO$ molecules are accommodated in each supercage of the zeolite at saturation. It appears

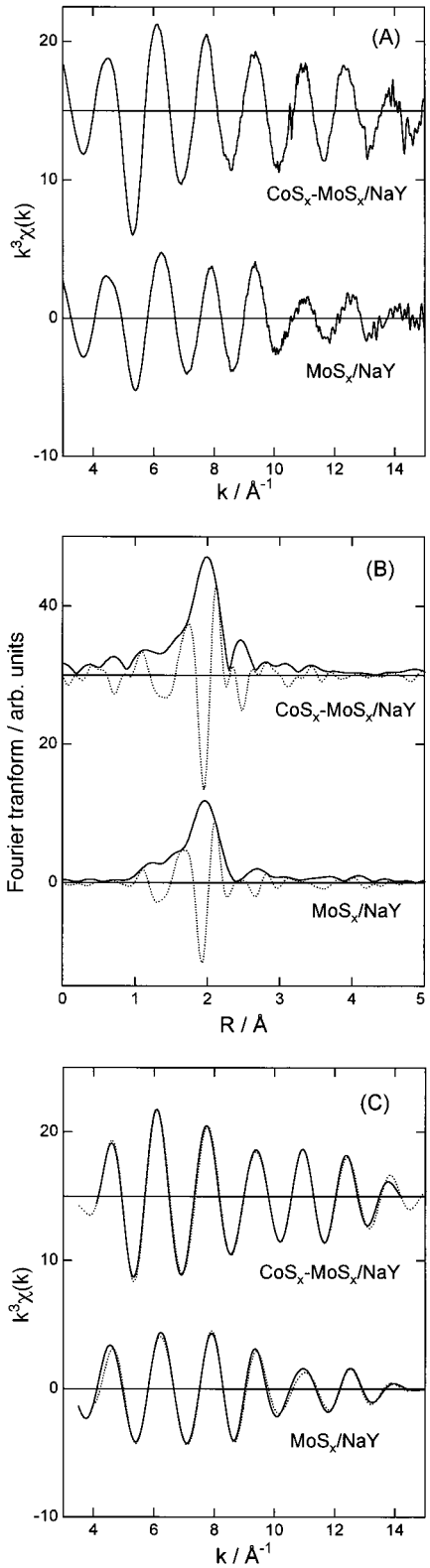


**Figure 1.** EXAFS results for the Mo K-edge of MoSx/NaY and CoSx−MoSx/NaY sulfided for 1.5 h: (A) $k^3$-weighted EXAFS oscillation; (B) $k^3$-weighted Fourier transform ($\Delta k$ = 3.28−14.58 Å$^{-1}$ for MoSx/NaY and $k$ = 4.02−14.92 Å$^{-1}$ for CoSx−MoSx/NaY); (C) Fourier filtered EXAFS function ($k^3$, solid line (observed); $k^3$, dotted line (calculated), $\Delta R$ = 1.35−3.33 Å, $\Delta k$ = 4.08−14.42 Å$^{-1}$ for MoSx/NaY and $\Delta R$ = 1.35−3.25 Å, $\Delta k$ = 4.13−14.22 Å$^{-1}$ for CoSx−MoSx/NaY).

that during the present careful sulfidation procedures, two molecules are combined into stable dimer species in the supercage. According to Coddington et al.,[26] a thermal treatment

**TABLE 1: Structural Parameters As Derived from the EXAFS Analysis Using FEFF Parameters for Mo, Co, and Co−Mo Sulfide Clusters Encaged in an NaY Zeolite[a]**

| catalyst | absorber−scatterer pair | $R$/nm | CN | $E_0$/eV | $\Delta\sigma^2$/Å$^2$ |
|---|---|---|---|---|---|
| MoSx/NaY[b,c] | Mo−S | 0.240 | 4.7 | −2.3 | 0.0048 |
| | Mo−Mo | 0.315 | 1.1 | −2.0 | 0.0089 |
| MoSx/NaY[c] | Mo−S | 0.240 | 3.8 | 2.4 | 0.0028 |
| | Mo−Mo | 0.313 | 0.8 | −5.6 | 0.0045 |
| CoSx/NaY[c] | Co−S | 0.223 | 5.7 | 4.8 | 0.0070 |
| | Co−Co | 0.254 | 0.7 | 0.8 | 0.0001 |
| CoSx−MoSx/NaY[c] | Mo−S | 0.241 | 4.4 | 0.7 | 0.0012 |
| | Mo−Co | 0.281 | 1.7 | 4.0 | 0.0064 |
| | Mo−Mo | 0.322 | 0.9 | 0.9 | 0.0072 |
| | Co−S | 0.223 | 3.4 | 3.5 | 0.0025 |
| | Co−Co | 0.254 | 0.7 | −2.7 | 0.0085 |
| | Co−Mo | 0.282 | 1.7 | 9.5 | 0.0096 |
| CoSx−MoSx/NaY[d] | Mo−S | 0.241 | 4.7 | 2.3 | 0.0017 |
| | Mo−Co | 0.281 | 2.2 | 5.6 | 0.0092 |
| | Mo−Mo | 0.322 | 0.9 | 1.6 | 0.0070 |
| CoSx/MoSx/NaY[c] | Mo−S | 0.241 | 4.0 | 5.0 | 0.0014 |
| | Mo−Co | 0.280 | 1.1 | −0.2 | 0.0054 |
| | Mo−Mo | 0.321 | 0.5 | −3.2 | 0.0054 |

[a] $R$, distance; CN, coordination number; $E_0$, inner potential, $\Delta\sigma^2$, relative Debye−Waller-like factor. [b] Empirical parameters. [c] Sulfided for 1.5 h. [d] Sulfided for 20 h.

of $Mo(CO)_6$/NaY in a vacuum produced Mo metal dimer species, $Mo_2$, encaged in the supercage of the zeolite. Mo oxide dimer species were also reported to form from $Mo(CO)_6$/NaY by a mild thermal oxidation at 353−373 K or by photooxidation using gaseous oxygen.[27] Very recently, Asakura et al.[28] found the formation of $Mo_2C$ clusters by decarbonylation of $Mo(CO)_6$/NaY at 523 K.

CoSx−MoSx/NaY (2 Mo/SC) was found to show catalytic synergies between Co and Mo sulfides for the HDS of thiophene and to exhibit the highest activity at the composition of Co/Mo = 1.[20] The catalytic activity was not altered at all even after a 20 h treatment of the catalyst at 673 K in a stream of $H_2S/H_2$, indicating a high thermal stability of the catalytically active species. The product selectivity of CoSx−MoSx/NaY ((2Co + 2Mo)/SC) for the hydrogenation of butadiene was very close to that of CoSx/NaY (2 Co/SC) despite the simultaneous presence of the same amounts of Co and Mo, suggesting that the reaction takes place exclusively on the Co sites.[20] These catalytic properties cannot be understood in terms of a simple physical mixture of Co and Mo sulfide clusters. Alternatively, these results indicate formation of thermally stable and catalytically active Co−Mo binary sulfide clusters. In contrast to CoSx−MoSx/NaY, no obvious catalytic synergy was observed for CoSx/MoSx/NaY prepared using $Co_2(CO)_8$ instead of $Co(CO)_3NO$.[20]

The formation of Co−Mo binary sulfide clusters in the Co−Mo binary sulfide catalyst was examined by XPS. Figures 3 and 4 show the XP spectra of the Mo 3d and Co 2p levels, respectively, for the MoSx/NaY, CoSx/NaY, and CoSx−MoSx/NaY sulfided for 1.5 h. The Mo $3d_{5/2}$ binding energies for MoSx/NaY (229.2 eV) and CoSx−MoSx/NaY (229.2) are consistent with those for polycrystalline $MoS_2$ (229.2) and for supported Mo sulfide species.[29] The Co $2p_{3/2}$ binding energy for CoSx/NaY is 778.5 eV, in agreement with that for $Co_9S_8$ (778.4 eV) and sulfided Co species.[30] However, CoSx−MoSx/NaY shows a Co $2p_{3/2}$ band at 779.3 eV, which is higher by 0.8−0.9 eV than that for CoSx/NaY or $Co_9S_8$. Alstrup et al.[31] reported a high Co $2p_{3/2}$ binding energy for the Co−Mo−S phase (779.0 eV) in Co−Mo/$Al_2O_3$ catalysts compared to that for $Co_9S_8$ (778.4). The asymmetric spectral features of the Co 2p bands, due to final state effects,[31,32] are also very close to those reported

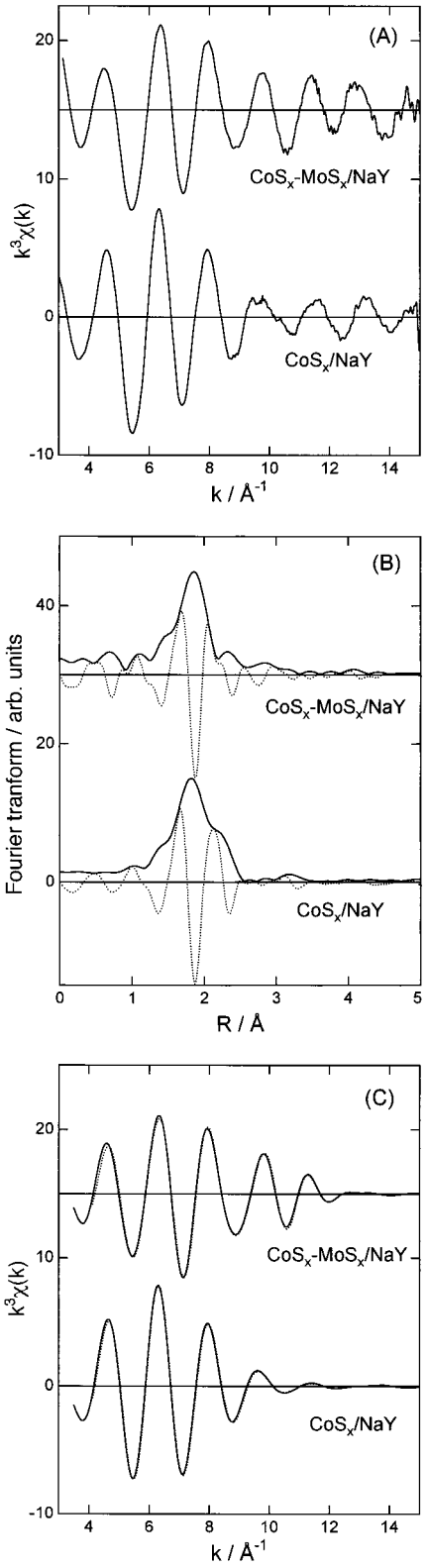


**Figure 2.** EXAFS results for the Co K-edge of CoSx/NaY and CoSx−MoSx/NaY sulfided for 1.5 h: (A) $k^3$-weighted EXAFS oscillation; (B) $k^3$-weighted Fourier transform ($\Delta k$ = 3.29−14.39 Å$^{-1}$ for CoSx/NaY and $\Delta k$ = 3.36−14.37 Å$^{-1}$ for CoSx−MoSx/NaY); (C) Fourier filtered EXAFS function ($k^3$, solid line (observed); $k^3$, dotted line (calculated), $\Delta R$ = 1.24−2.67 Å, $\Delta k$ = 4.10−11.90 Å$^{-1}$ for CoSx/NaY and $\Delta R$ = 1.35−3.13 Å, $\Delta k$ = 4.10−11.70 Å$^{-1}$ for CoSx−MoSx/NaY).

for the Co−Mo−S phase.[31] Accordingly, it is concluded that the Co sulfide species chemically interact with the Mo sulfide species to form Co−Mo binary sulfide clusters in CoSx−MoSx/NaY. The unaltered binding energy of the Mo 3d level on the addition of Co may be due to coincidental compensation of initial and final state effects.[32]

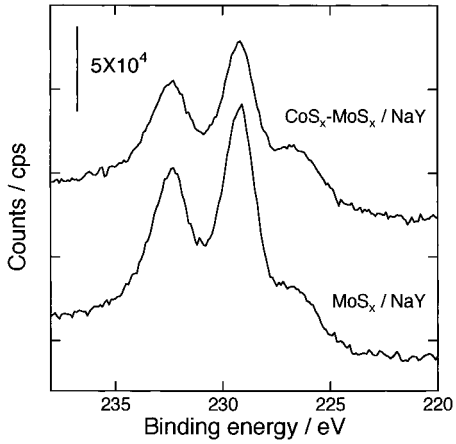


**Figure 3.** Mo 3d XP spectra for MoSx/NaY and CoSx−MoSx/NaY sulfided for 1.5 h.

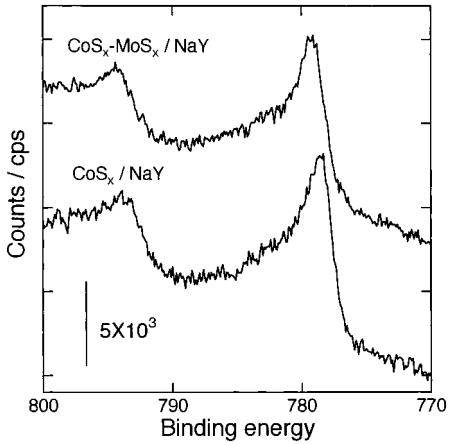


**Figure 4.** Co 2p XP spectra for CoSx/NaY and CoSx−MoSx/NaY sulfided for 1.5 h.

**TABLE 2: Compositions of MoSx/NaY, CoSx/NaY, CoSx−MoSx/NaY, and CoSx/MoSx/NaY Catalysts**

| | metal atoms/SC | | | |
|---|---|---|---|---|
| catalyst | Mo | Co | composition | technique |
| MoSx/NaY | 2.0[a] | | $MoS_{1.9-2.0}$ | XPS |
| | 1.9 | | $MoS_{2.1}$ | XRF |
| CoSx/NaY | | 2.1 | $CoS_{1.0}$ | XRF |
| CoSx−MoSx/NaY | 2.0[a] | 2.0[a] | $Co_{2.0}Mo_{2.0}S_{5.8}$ | XPS |
| | 1.9 | 2.0 | $Co_{2.0}Mo_{1.9}S_{5.7}$ | XRF |
| CoSx/MoSx/NaY | 1.2[a] | 2.0[a] | | |

[a] Chemical analysis using ICP and AAS. Accuracy: ±0.1/SC.

It is considered that the Co−Mo binary sulfide clusters formed in CoSx−MoSx/NaY are located inside the supercage of the zeolite, since Mo sulfide clusters are present in the pores before the introduction of Co.[20] On the other hand, it was shown previously by XPS[20] that with CoSx/MoSx/NaY ((1.2Co + 2Mo)/SC) prepared from $Co_2(CO)_8$, a part of the Co species was segregated on the external surface of MoSx/NaY zeolite particles, forming separate Co sulfide species (Co $2p_{3/2}$; 778.4 eV).

The composition of the Co−Mo binary sulfide clusters was estimated by XRF and XPS techniques. The catalyst compositions are summarized in Table 2. In the case of the XPS analysis, the S 2p (S 2s)/Mo 3d XPS intensity ratio normalized to that for $MoS_2$ was used to calculate the composition of the clusters,

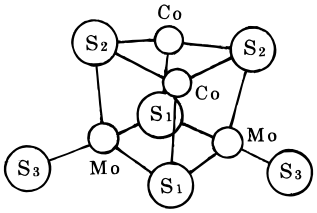


**Figure 5.** Thiocubane structure proposed for $Co_2Mo_2S_6$ clusters. The number attached to the sulfur atom corresponds to that in Table 3.

combined with the composition from chemical analysis. Table 2 clearly indicates that the compositions obtained by XRF and XPS are in excellent agreement with each other. It should be noted that XRF provides a bulk composition, while XPS gives a surface one. Accordingly, it is considered that Co, Mo, and S are homogeneously distributed throughout the zeolite pores. Taking into consideration that two Co and two Mo atoms are accommodated (on average) in the supercage of the host zeolite, it is concluded that the composition of the intrazeolite Co−Mo binary sulfide clusters is $Co_2Mo_2S_6$.

The structure of $Co_2Mo_2S_6$ clusters was determined by EXAFS techniques. The $k^3$-weighted EXAFS oscillations and Fourier transforms of Mo and Co K-edges for CoSx−MoSx/NaY are presented in Figures 1 and 2, respectively. By comparison of the Mo K-edge Fourier transform for MoSx/NaY, it is evident that CoSx−MoSx/NaY shows a small but new peak at ca. 0.24 nm (no phase shift corrected) in addition to those due to Mo−S (ca. 0.20 nm) and Mo−Mo (ca. 0.28 nm) bondings. It is found that the Fourier transform ($\Delta R = 0.135-0.324$ nm) including the peak at ca. 0.24 nm is satisfactorily curve-fitted only by assuming S, Co, and Mo as scatterers. The interatomic distance of Mo−Co bondings is calculated to be 0.281 nm as summarized in Table 1. Similarly, Figure 2 indicates an appearance of a new Co K-edge Fourier transform peak at ca. 0.23 nm, which is curve-fitted only by Co−Mo bondings, in the presence of Mo sulfide clusters. The interatomic distance of Co−Mo bondings is calculated to be 0.282 nm, in excellent agreement with that from the Mo K-edge EXAFS. The coordination numbers of the Mo−Co and Co−Mo bondings, which are calculated from the Mo and Co K-edge EXAFS, respectively, are consistent with each other and are about 2. Taking into consideration the coordination numbers of the Mo−Mo, Mo−S, Co−Co, and Co−S bondings in Table 1, the structure of $Co_2Mo_2S_6$ clusters is proposed to be of a thiocubane type as illustrated in Figure 5. The Co atom is coordinated by three sulfur atoms, while the Mo atom is surrounded by four sulfur atoms. It is worth noting that the Mo−Co interatomic distance is very close to that reported for a Co−Mo−S phase supported on activated carbon[33] or metal oxides.[34]

The $k^3$-weighted Fourier transforms of Mo K-edge EXAFS spectra for CoSx−MoSx/NaY ((2Co + 2Mo)/SC) sulfided at 673 K for 20 h and CoSx/MoSx/NaY ((1.2Co + 2Mo)/SC) are compared in Figure 6 with those for MoSx/NaY and CoSx−MoSx/NaY sulfided for 1.5 h. The structural parameters as derived from the EXAFS analysis are also summarized in Table 1. It is evident that with CoSx−MoSx/NaY, the prolonged sulfidation essentially does not change the Fourier transform and the structural parameters, clearly demonstrating high thermal stability of $Co_2Mo_2S_6$ clusters. This is in accord with the findings[20] that the HDS activity of CoSx−MoSx/NaY is not altered at all by the prolonged sulfidation at 673 K. On the other hand, a Fourier transform peak due to Mo−Co bondings (ca. 0.24 nm) is apparently weaker for CoSx/MoSx/NaY than that for CoSx−MoSx/NaY. The low Mo−Co coordination number in Table 1 for CoSx/MoSx/NaY indicates that only part of the

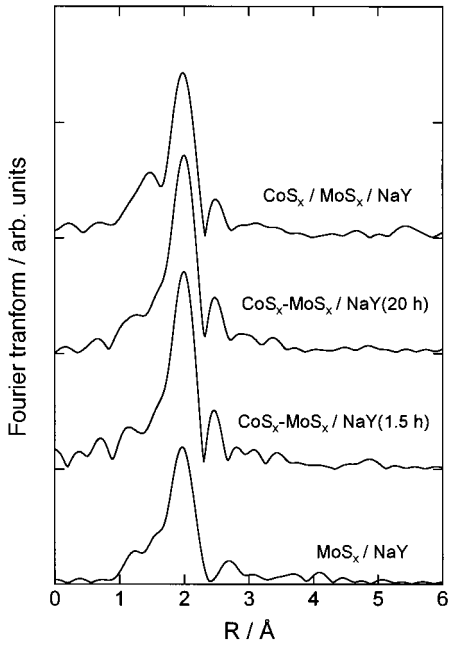


**Figure 6.** $k^3$-weighted Mo K-edge Fourier transforms for MoSx/NaY ($\Delta k = 3.28-14.58$ Å$^{-1}$), CoSx−MoSx/NaY sulfided for 1.5 h ($\Delta k = 4.02-14.92$ Å$^{-1}$), CoSx−MoSx/NaY sulfided for 20 h ($\Delta k = 4.07-14.92$ Å$^{-1}$), and CoSx/MoSx/NaY ($\Delta k = 3.38-14.62$ Å$^{-1}$).

**TABLE 3: Theoretical Interatomic Distances for a $Co_2Mo_2S_6$ Cluster**[a]

| atom pair | interatomic distance/nm |
|---|---|
| Mo−$S_1$ | 0.242 |
| Mo−$S_2$ | 0.239 |
| Mo−$S_3$ | 0.216 |
| Co−$S_2$ | 0.219 |
| Co−$S_1$ | 0.217 |
| Mo−Mo | 0.298 |
| Co−Co | 0.266 |
| Mo−Co | 0.256 |

[a] The number attached to the S atom; see Figure 5.

Mo sulfide species is converted to $Co_2Mo_2S_6$ clusters, mostly as a consequence of the lower Co content in the catalyst (1.2 Co/SC vs 2 Co/SC). The rest of the Mo sulfide species remains intact as separate Mo sulfide clusters. Taking into consideration the XPS results[20] showing a surface segregation of Co sulfide species, it is conjectured that a small part of Co sulfide species segregates on the external surface of the catalyst, while most of $Co_2(CO)_8$ and/or Co species formed by the decomposition of $Co_2(CO)_8$ molecules diffuse into the zeolite pores and react with the Mo sulfide species to form $Co_2Mo_2S_6$ clusters. The surface Co sulfide phase may retard the reactants, such as thiophene, in diffusing into the zeolite pores and in reaching the catalytically active $Co_2Mo_2S_6$ clusters. This may explain the relatively low catalytic activity of CoSx/MoSx/NaY for the HDS of thiophene.[20]

To examine the possibility of the formation of the thiocubane clusters, DF calculations were performed for the $Co_2Mo_2S_6$ structure proposed in Figure 5. The structure was optimized under the $C_{2v}$ symmetry constraint using the same functionals as the SCF calculations. The optimized structure thus obtained is still of a thiocubane type, and the theoretical interatomic distances are summarized in Table 3. Accordingly, the theoretical results strongly suggest thermodynamical stability of the thiocubane cluster in Figure 5. It appears, however, that the theoretical interatomic distances are not in very good agreement

with those in Table 1 obtained from the EXAFS analyses. The major discrepancies in the experimental and theoretical bond distances are considered to be a consequence of the interactions between $Co_2Mo_2S_6$ clusters and zeolite frameworks, since the theoretical calculations were conducted for a free $Co_2Mo_2S_6$ molecule.

In homogeneous reaction systems, thiocubane type $Co_2Mo_2$ sulfide clusters are synthesized in several ways.[35−40] For instance, according to Curtis et al.,[40] a Mo sulfide dimer complex, $Cp'_2Mo_2S_4$, reacts with $Co_2(CO)_8$, producing $Cp'_2Mo_2Co_2S_4(CO)_2$ in high yield. A reaction of $Mo_2S_4(S_2CNEt_2)_2$ with $Co_2(CO)_8$ also produces a thiocubane complex with a $Co_2Mo_2S_4$ core by oxidative addition of Co.[39] These well-established reactions in homogeneous systems strongly suggest that the formation of the intrazeolite $Co_2Mo_2S_6$ thiocubane clusters is rational, since Mo dimer clusters are formed in the pores before the introduction of $Co(CO)_3NO$. The extremely high thermal stability of the $Co_2Mo_2S_6$ clusters (no HDS activity or structural changes at 673 K) may be ascribed to specific interactions of the clusters with the framework of the host zeolite, which can be regarded as solid ligands or solid solvent.[41]

In the case of $Al_2O_3$ as a host material, we failed to prepare Co−Mo binary sulfide clusters possessing a well-defined structure.[42] Mo sulfide dimer clusters were not thermally stabilized on the $Al_2O_3$ surface and easily agglomerated into larger Mo sulfide clusters having a $MoS_2$ structure at 673 K. Analogous observations were reported by Curtis et al.[18] for $Al_2O_3$-supported $Cp_2Mo_2Co_2S_3(CO)_4$; Co K-edge XANES showed that the cluster complex was degraded after the adsorption on $Al_2O_3$ even at RT. In the case of Fe−Mo binary sulfide complex supported on $Al_2O_3$,[18] a complete decomposition of the cluster was concluded by an EXAFS study after heating at 393 K. The high thermal stabilities of the intrazeolite Mo and Co sulfide dimer clusters and $Co_2Mo_2S_6$ binary sulfide clusters are considered to be a consequence of nondestructive interactions with the zeolite frameworks, such as coordinations of framework oxygens to coordinatively unsaturated Mo and/or Co atoms, which in the present study we could not specify by using EXAFS spectra measured at RT though. The high coordinative unsaturations of Mo and Co in the Mo, Co, and Co−Mo sulfide clusters were evidenced by their high NO adsorption capacities.[43]

## Conclusions

The structure of the intrazeolite Co−Mo binary sulfide clusters, prepared from $Mo(CO)_6$ and $Co(CO)_3NO$ as the precursors, was studied by means of XPS and EXAFS. The Co 2p XPS and Mo and Co K-edge EXAFS clearly show the formation of the clusters. It is concluded that the composition of the clusters is $Co_2Mo_2S_6$ on the basis of XPS and XRF analyses. It is strongly suggested by Mo and Co K-edge EXAFS analysis using FEFF parameters that the structure of $Co_2Mo_2S_6$ clusters is of thiocubane type. The thiocubane structure is rationalized by the theoretical calculations using a density functional method. It is concluded that the intrazeolite Co−Mo binary sulfide clusters are $Co_2Mo_2S_6$ possessing a thiocubane structure thermally stabilized by interactions with the framework of the host zeolite. It is shown by EXAFS that the Co−Mo sulfide catalyst prepared by using $Co_2(CO)_8$ consists of three phases: Co sulfides segregated on the outer surface of the catalyst, intrazeolite Mo sulfide clusters, and $Co_2Mo_2S_6$ binary sulfide clusters.

**Acknowledgment.** This work was supported by a Grant-in-Aid for Scientific Research from the Ministry of Education, Science, Sports and Culture (09650860) of Japan. This work was also supported by CREST, Japan Science and Technology Corporation. The present authors are very grateful to Prof. T. Tanaka (Kyoto University) for measuring some of the EXAFS data and to Prof. K. Tatsumi (Nagoya University) for stimulating discussions.

**Supporting Information Available:** Orbital basis sets used in the present density functional calculation. This material is available free of charge via the Internet at http://pubs.acs.org.

## References and Notes

(1) Gates, B. C.; Katzer, J. R.; Schuit, G. C. A. *Chemistry of Catalytic Processes*; McGraw-Hill: New York, 1979; p 390. Schuit, G. C. A.; Gates, B. C. *ALChE J*. **1973**, *19*, 417.

(2) Topsøe, H.; Clausen, B. S.; Massoth, F. E. *Catalysis: Science and Technology*; Anderson, J. R., Boudard, M., Eds.; Springer-Verlag: Berlin, 1996; Vol. 11, p 1.

(3) Topsøe, H.; Clausen, B. S. *Catal. Rev. Sci. Eng*. **1984**, *26*, 395. Topsøe, H.; Clausen, B. S.; Topsøe, N.; Pederson, E. *Ind. Eng. Chem. Fundam*. **1986**, *25*, 25.

(4) Chianelli, R. R. *Cata,. Rev. Sci. Eng*. **1984**, *26*, 361.

(5) Prins, R.; de Beer, V. H. J.; Somorjai, G. A. *Catal. Rev. Sci. Eng*. **1989**, *31*, 1.

(6) Delmon, B. *Catal. Lett*. **1993**, *22*, 1.

(7) Chianelli, R. R.; Daage, M.; Ledoux, M. J. *Adv. Catal*. **1994**, *40*, 177.

(8) Startsev, A. N. *Catal. Rev. Sci. Eng*. **1995**, *37*. 353.

(9) Clausen, B. S.; Mørup, S.; Topsøe, H.; Candia, R. *J. Phys., Colloq*. **1976**, *37*, C6−C249. Topsøe, H.; Clausen, B. S.; Candia, R.; Wivel, C.; Mørup, S. *J. Catal*. **1981**, *68*, 433. Wivel, C.; Candia, R.; Clausen, B. S.; Mørup, S.; Topsøe, H. *J. Catal*. **1982**, *68*, 453. Topsøe, H.; Clausen, B. S.; Candia, R.; Wivel, C.; Mørup, S. *Bull. Soc. Chim. Belg*. **1981**, *90*, 1189. Topsøe, N.; Topsøe, H. *J. Catal*. **1983**, *84*, 386.

(10) Stiefel, E. I.; Halbert, T. R.; Coyle, C. L.; Wei, L.; Pan, W.-H.; Ho, T. C.; Chianelli, R. R.; Daage, M. *Polyhedron* **1989**, *8*, 1625.

(11) Angelici, R. J. *Acc. Chem. Res*. **1988**, *21*, 387. Jones, W. D.; Chin, R. M. *J. Am. Chem. Soc*. **1994**, *116*, 198. Bianchini, C.; Meli, A.; Perzzini, M.; Vizza, F.; Moneti, S.; Herrerra, V.; Sanchez-Delgado, R. A. *J. Am. Chem. Soc*. **1994**, *116*, 4370.

(12) Casewit, C. J.; Rakowski DuBois, M. *J. Am. Chem. Soc*. **1986**, *108*, 5482.

(13) Riaz, U.; Curnow, O. J.; Curtis, M. D. *J. Am. Chem. Soc*. **1991**, *113*, 1416. Curnow, O. J.; Kampf, J. W.; Curtis, M. D.; Shen, J.-K.; Basolo, F. *J. Am. Chem. Soc*. **1994**, *116*, 224. Riaz, U.; Curnow, O. J.; Curtis, M. D. *J. Am. Chem. Soc*. **1994**, *116*, 4357. Druker, S. H.; Curtis, M. D. *J. Am. Chem. Soc*. **1995**, *117*, 6366.

(14) Curtis, M. D.; Druker, S. H. *J. Am. Chem. Soc*. **1997**, *119*, 1027.

(15) Dunker, S. H.; Curtis, M. D. *J. Am. Chem. Soc*. **1997**, *119*, 842.

(16) Bianchini, C.; Meli, A. *Acc. Chem. Res*. **1998**, *31*, 109.

(17) Eltzner, W.; Breysse, M.; Lacroix, M.; Vrinat, M. *Polyhedron* **1986**, *5*, 203.

(18) Curtis, M. D.; Penner-Hahn, J. E.; Schwank, J.; Baralt, O.; McCabe, D. J.; Thompson, L.; Waldo, G. *Polyhedron* **1988**, *7*, 2411. Curtis, M. D. *Appl. Organomet. Chem*. **1992**, *6*, 429.

(19) Carville, B. T.; Thompson, L. T. *Appl. Catal*. **1991**, *75*, 249. Song, C.; Parfitt, D. S.; Schobert, H. H. *Catal. Lett*. **1993**, *21*, 27.

(20) Okamoto, Y.; Katsuyama, H. *Stud. Surf. Sci. Catal*. **1996**, *101*, 503. Okamoto, Y.; Katsuyama, H. *AIChE J*. **1997**, *43*, 2809.

(21) Rehr, J. J.; Mustre de Leon, J.; Zabinsky, S. I.; Albers, R. C. *J. Am. Chem. Soc*. **1991**, *113*, 5135. O'Day, P. A.; Rehr, J. J.; Zabinsky, S. I.; Brown, G. E., Jr. *J. Am. Chem. Soc*. **1994**, *116*, 2838.

(22) St-Amant, A.; Salahub, D. R. *Chem. Phys. Lett*. **1990**, *169*, 387. Kobayashi, H.; Salahub, D. R.; Ito, T. *J. Phys. Chem*. **1994**, *98*, 5487.

(23) Becke, A. D. *Phys. Rev*. **1988**, *A38*, 3098.

(24) Perdew, J. P. *Phys. Rev*. **1986**, *B33*, 8822. Perdew, J. P. *Phys. Rev*. **1986**, *B34*, 7406.

(25) Okamoto, Y.; Katsuyama, H. *Ind. Eng. Chem. Res*. **1996**, *35*, 1834. Okamoto, Y.; Katsuyama, H.; Yoshida, K.; Nakai, K.; Matsuo, M.; Sakamoto, Y.; Yu, J.; Terasaki, O. *J. Chem. Soc., Faraday Trans*. **1996**, *92*, 4647. Sakamoto, Y.; Togashi, N.; Terasaki, O.; Ohsuna, T.; Okamoto, Y.; Hiraga, K. *Mater. Sci. Eng. A* **1996**, *217*/*218*, 147.

(26) Coddington, J. M.; Howe, R. F.; Asakura, K.; Iwasawa, Y. *J. Chem. Soc., Faraday Trans*. **1990**, *86*, 1015.

(27) Okamoto, Y.; Kobayashi, Y.; Imanaka, T. *Catal. Lett*. **1993**, *20*, 49.

(28) Asakura, K.; Noguchi, Y.; Iwasawa, Y. *J. Phys. Chem. B* **1999**, *103*, 1051.

(29) Patterson, T. A.; Carver, J. C.; Leyden, D. E.; Hercules, D. M. *J. Phys. Chem*. **1976**, *80*, 1700. Okamoto, Y.; Tomioka, H.; Katoh, Y.; Imanaka, T.; Teranishi, S. *J. Phys. Chem*. **1980**, *84*, 1833. de Jong, A. M.; Borg, H. J.; van Ijzendoorn, L. J.; Soudant, V. G. F.; de Beer, V. H. J.; van Veen, J. A. R.; Niemantsverdriet, J. W. *J. Phys. Chem*. **1993**, *97*, 6477.

(30) Okamoto, Y.; Imanaka, T.; Teranishi, S. *J. Catal*. **1980**, *65*, 448. Chin, R. L.; Hercules, D. M. *J. Phys. Chem*. **1982**, *86*, 3079. Okamoto, Y.; Nagata, K.; Imamaka, T.; Inamura, K.; Takyu, T. *Bull. Chem. Soc. Jpn*. **1992**, *65*, 1331.

(31) Alstrup, I.; Chorkendorff, I.; Candia, R.; Clausen, B. S.; Topsøe, H. *J. Catal*. **1982**, *77*, 397.

(32) Delgass, W. N.; Haller, G. L.; Kellerman, R.; Lunsford, J. H. *Spectroscopy in Heterogeneous Catalysis*; Academic Press: New York, 1979; p 267.

(33) Bouwens, S. M. A. M.; Prins, R.; de Beer, V. H. J.; Koningsberger, D. C. *J. Phys. Chem*. **1990**, *94*, 3711. Bouwens, S. M. A. M.; van Veen, J. A. R.; Koningsberger, D. C.; de Beer, V. H. J.; Prins, R. *J. Phys. Chem*. **1991**, *95*, 123.

(34) Bouwens, S. M. A. M.; van Zon, F. B. M.; van Dijik, M. P.; van der Kraan, A. M.; de Beer, V. H. J.; van Veen, J. A. R.; Koningsberger, D. C. *J. Catal*. **1994**, *146*, 375.

(35) Armstrong, W. H.; Marscharak, P. K.; Holm, R. H. *Inorg. Chem*. **1982**, *21*, 1701.

(36) Brunner, H.; Wachtere, J. *J. Organomet. Chem*. **1982**, *240*, C41. Brunner, H.; Kauermann, H.; Wachter, J. *Angew. Chem., Int. Ed. Engl*. **1983**, *22*, 549.

(37) Roberts, D. A.; Geoffroy, G. L. *Comprehensive Organometallic Chemistry*; Wilkinson, G., Stone, F. G. A., Abe, E. W., Eds.; Pergamon: Oxford, 1982; Vol. 6, p 763.

(38) Rauchfuss, T. B.; Weatherill, T. D.; Wilson, S. R.; Zebrowski, J. P. *J. Am. Chem. Soc*. **1983**, *105*, 6508.

(39) Halbert, T. R.; Cohen, S. A.; Stiefel, E. I. *Organometallics* **1985**, *4*, 1689.

(40) Curtis, M. D. *Polyhedron* **1987**, *6*, 759. Curtis, M. D.; Willams, P. D.; Butler, W. M. *Inorg. Chem*. **1988**, *27*, 2853. Li, P.; Curtis, M. D. *Inorg. Chem*. **1990**, *29*, 1242.

(41) Ozin, G. A.; Gil, C. *Chem. Rev*. **1989**, *89*, 1749.

(42) Okamoto, Y.; Odawara, M.; Onimatsu, H,; Imanaka. *Ind. Eng. Chem. Res*. **1995**, *34*, 3707.

(43) Okamoto, Y.; Maezawa, A.; Kane, H.; Imanaka, T. *J. Mol. Catal*. **1989**, *52*, 337. Okamoto, Y.; Kubota, T. Unpublished results.